Supplementary Movie Legends

Movie S1 Recruitment of Tie2 at cell-cell contacts upon COMP-Ang1 stimulation. Confluent HUVECs plated on collagen-coated glass base dish were transfected with the plasmid encoding Tie2-GFP and that encoding HcRed-p120 catenin, starved for 3 h, and stimulated with COMP-Ang1 (200 ng ml^{-1}). A series of GFP image (left) and HcRed (right) images were saved as a stack file, which was converted to a video file. Elapsed time is indicated as h : min.

Movie S2 Internalisation of ectopic Tie2 upon COMP-Ang1 stimulation in the absence of cell-cell contacts between the cells ectopically expressing Tie2. CHO cells transfected with the plasmid expressing Tie2-GFP were plated on collagen-coated dish, starved for 3 h, and stimulated with COMP-Ang1 (200 ng ml^{-1}). A series of GFP images (left) and phase-contrast images (right) were saved as a stack file, which was converted to a video file. Elapsed time is indicated as h: min. Note that Tie2-GFP-expressing cells are surrounded by those that do not express Tie2-GFP.

Movie S3 *Trans*-association of Tie2 at cell-cell contacts upon COMP-Ang1 stimulation. CHO cells transfected with the plasmid expressing Tie2-GFP were stimulated with COMP-Ang1 and time-lapse imaged similarly to the legend of Movie S2. Note that Tie2-GFP-expressing cells contact each other.

Movie S4 *Trans*-association of Tie2 at cell-cell contacts does not need the cytoplasmic domain of Tie2. CHO cells transfected with the plasmid expressing Tie2Δcyto-GFP were stimulated with COMP-Ang1 and time-lapse imaged similarly to the legend of Movie S2.

Movie S5 Sparse HUVECs plated on a collagen-coated dish were transfected with the plasmid encoding Tie2-GFP and that encoding RFP-Crk, starved for 3 h, and stimulated with COMP-Ang1 (200 ng ml^{-1}). Fluorescence images of GFP and RFP simultaneously recorded were merged at each time point. A series of GFP (top) and merged images (bottom) were saved as stack files, which were converted to video files. The boxed areas in the left movies are enlarged on the right side. Note that Tie2-GFP is accumulated at the extended membrane close to RFP-Crk-marked focal complexes as indicated by arrow. Tie2-GFP remains at the initial accumulation site at cell-substratum even after RFP-Crk detaches from initial focal complexes. Elapsed time is indicated as h: min.

Movie S6 Sparse CHO cells plated on a collagen-coated dish were transfected with the plasmid encoding Tie2-GFP and that encoding RFP-Crk, starved for 3 h, and stimulated with COMP-Ang1 (200 ng ml^{-1}). Fluorescence images of GFP and RFP and phase-contrast images were simultaneously recorded. GFP and RFP images were merged at each time point. A series of GFP (top left), RFP (top right), merged (bottom left) and phase-contract (bottom right) images were saved as stack files, which were converted to video files. Note that Tie2-GFP is accumulated at cell periphery close to RFP-Crk-marked focal complexes, and remains at the initial accumulation site even after RFP-Crk detaches from initial focal complexes. Elapsed time is indicated as h: min.

Movie S7 Sparse CHO cells expressing Tie2Δcyto-GFP and RFP-Crk were stimulated with COMP-Ang1 and time-lapse imaged similar to that described in the legend of Movie S6. Note that similar to Tie2-GFP, Tie2Δcyto-GFP is also targeted to cell periphery close to RFP-Crk-marked focal complexes, and stabilised at initial accumulation site.

SUPPLEMENTARY INFORMATION

SUPPLEMENTARY METHODS

Reagents and antibodies. COMP-Ang1, Ang1, GCN4-Ang1 and MAT-Ang1 were prepared as N-terminally Flag-tagged proteins as described before [1]. VEGF, sTie2-Fc and sTie1-Fc were purchased from R & D systems (Minneapolis, MN). Anti-GFP antibody was generated as described previously [2]. Other antibodies used here were purchased as follows: anti-Tie2 and anti-VE-cadherin from Santa Cruz Biotechnology (Santa Cruz, CA); anti-VE-cadherin, anti-PECAM-1, anti-β-catenin, anti-paxillin, anti-β3 integrin, anti-FAK, anti-VASP and anti-eNOS from BD bioscience (San Jose, CA); anti-HA from Roche Applied Science; anti-Flag (M2), anti-vinculin, anti-β-actin and anti-talin from Sigma-Aldrich; anti-α5 integrin and anti-fibronectin from Chemicon International Inc. (Temecula, CA); anti-phosphotyrosine (PY100), anti-Erk, anti-phospho-Erk, anti-Akt, anti-phospho-Akt, anti-VEGFR2, anti-Foxo1, anti-phospho-Foxo1 and anti-phospho-eNOS from Cell Signaling Technology (Beverly, MA); anti-phosphoTie2 ($pTyr^{1102/1108}$) from Calbiochem (San Diego, CA); anti-Tie2 (TEK4) from eBioscience (San Diego, CA); horseradish peroxidase-coupled sheep anti-mouse, anti-rabbit and anti-goat IgG from GE Healthcare Life Science; Alexa 488- or Alexa 546-labeled secondary antibodies from Molecular Probes (Eugene, OR). Rhodamine-phalloidin was purchased from Molecular Probes.

Plasmids and adenoviruses. A pcDNA-Tie2 plasmid encoding full-length murine Tie2 was kindly provided by T. Suda (Keio University, Tokyo, Japan). cDNA fragments encoding full-length mTie2 and its deletion mutant lacking the cytoplasmic region (amino acids 1-810) amplified by PCR using pcDNA-Tie2 as a template were inserted into pEGFP-N1 vector (Clontech, Mountain View, CA), namely pEGFP-N1-Tie2 and pEGFP-N1-Tie2Δcyto plasmids. A cDNA fragment encoding Tie2 lacking the cytoplasmic region tagged with GFP and that encoding Tie2 lacking cytoplasmic domain tagged with HA was inserted into pIRESneo vector (Clontech) to construct pIRESneo-Tie2Δcyto-GFP plasmid and pIRESneo-Tie2Δcyto-HA plasmid, respectively. pEGFP-N1-Tie2KD vector encoding a kinase-deficient mutant of Tie2 (K854R) was generated

using QuickChange Site-directed Mutagenesis kit (Stratagene, La Jolla, CA). To generate the plasmid expressing the secreted form of the extracellular domain of Tie2 (amino acids 1-744) fused with HA tag followed by a six-His tag (sTie2-HA), a DNA fragment encoding sTie2-HA was amplified by PCR and inserted to pcDNA3.1 vector (Invitrogen Corp.). To construct pCMV-Tie2-HA and pCMV-Tie2Δcyto-HA vectors, cDNA fragment encoding EGFP was replaced with cDNA encoding HA tag in pEGFP-N1-Tie2 and pEGFP-N1-Tie2Δcyto vectors, respectively. To construct pVEGFR2-IRES-EGFP vector, a cDNA fragment encoding full-length VEGFR2 was amplified by PCR using BCMGSneo-KDR as a template [3] and inserted into pIRES2-EGFP vector (Clontech). For the preparation of a plasmid expressing RFP-FAT, cDNA fragment encoding RFP and that expressing FAT region of FAK (amino acids 885-1052) were PCR-amplified and sequentially inserted into pCXN2 vector [4]. pHcRed-p120 catenin and pCA-RFP-CrkI expressed HcRed tagged-p120 catenin and RFP-tagged CrkI, respectively [2,4]. pGFP-tensin encoding GFP-tagged chicken tensin was generously provided by K.M. Yamada (National Institute of Health)[5]. To generate pEGFP-C1-Foxo1 vector, a cDNA encoding Foxo1 was amplified by PCR using a Foxo1-expressing plasmid, kindly provided by A. Fukamizu (University of Tsukuba, Tsukuba, Japan)[6], as a template, and inserted into pEGFP-C1 vector (Clontech). A cDNA fragment encoding GFP-tagged FAT amplified by PCR was subcloned into pAdeno-X vector (Clontech), and the adenovirus was produced by using the Adeno-X system according to the manufacturer's protocol (Clontech). A recombinant adenovirus vector encoding constitutively active form of Foxo1was kindly provided by J. Nakae (Kobe University Graduate School of Medicine, Kobe, Japan)[7].

Cell culture, transfection, siRNA-mediated protein knockdown, and adenovirus infection. HUVECs and HAECs were purchased from Kurabo, and maintained as described previously [8]. CHO cells were cultured in nutrient mixture F-12 HAM media (Sigma) supplemented with 10% FCS. 293F cells were cultured in Free Style 293 expression media (Invitrogen Corp.) according to manufacturer's protocol. 293T cells were maintained in DMEM (Nissui) supplemented with 10% FCS. BaF3 cells and BaF-Tie2 cells (BaF3 cells stably expressing Tie2) were maintained in RPMI1640

supplemented with 10% FCS and 2 ng ml^{-1} murine IL3 as described before [9]. HUVECs were transfected with Lipofectamine 2000 reagent (Invitrogen Corp.), and both CHO and 293T cells were transfected with Lipofectamine Plus reagents (Invitrogen Corp.). 293F cells were transfected by using 293 fectin reagent (Invitrogen Corp.). Stealth siRNAs targeted to human α5-integrin (HSS105535, HSS105536), human β3 integrin (HSS105565, HSS105567), human VE-cadherin (HSS 101681, HSS101682), human PECAM-1 (HSS107803, HSS107804), human Tie2 (HSS110623, HSS110624) and human FAK (HSS108799, RNAi Duplex1 (Oligo ID12938-040)) were purchased from Invitrogen Corp. Tie2 siRNA (sc-36677) was obtained from Santa Cruz Biotechnology. As a control, siRNA duplex with irrelevant sequences was used. HUVECs were transfected with 20 nM siRNA duplexes using Lipofectamine 2000 reagent according to the manufacturer's instructions. After incubation for 48 h, the cells were used for the experiments. HUVECs were infected with adenoviruses at the appropriated multiplicities of infection for 12 h, and replaced with virus-free culture media. After additional culture for 24-48 h, the cells were used for the experiments.

Generation of BaF3 transfectant. To establish BaF3 cells stably expressing Tie2Δcyto-GFP (BaF-Tie2Δcyto-GFP) and the cells stably expressing Tie2Δcyto-HA (BaF-Tie2Δcyto-HA), a pIRESneo-Tie2Δcyto-GFP plasmid and a pIRESneo-Tie2Δcyto-HA plasmid were transfected into BaF3 cells by electroporation. Transfectants were selected with 600 μg ml^{-1} G418 (Invitrogen Corp.) for 2 weeks, then stained with anti-Tie2 antibody, and sorted by fluorescence-activated cell sorting analysis using FACSAria Cell-Sorting System (BD bioscience) to obtain the cells expressing comparable level of Tie2. Sorted cells were maintained in the presence of 400 μg ml^{-1} G418.

Ang1-ECM binding assay. Glass-base dishes were coated with 20 μg ml^{-1} BSA, fibronectin, vitronectin, laminin, and fibrinogen in PBS, or 0.15 mg ml^{-1} collagen type-I (Nitta Gelatin Inc., Osaka, Japan) in 1 mM HCl at 4 °C overnight. After washing with PBS, dishes were blocked with Block Ace (Dainippon Pharmaceuticals, Osaka, Japan) for 2 h at RT, and subsequently with 1% heat-inactivated BSA (at 85 °C for 12 min) in PBS for 2 h at 37 °C. The dishes were then incubated with 400 ng ml^{-1} Ang1, COMP-

Ang1, and Flag-tagged bacterial alkaline phosphatase (BAP) protein (Sigma-Aldrich) as a negative control in medium 199 containing 1% BSA for 1 h at 37 °C, and washed five times with PBS. Ang1, COMP-Ang1, and BAP protein bound to the dishes were detected by staining with anti-Flag antibody, and visualized with Alexa 546-labeled secondary antibody as described above. Average fluorescence intensity of ten random fields per dish was measured using MetaMorph 6.1 software.

Detection of Tie2, Erk, Akt, Foxo1 and eNOS phosphorylation. HUVECs placed on collagen-coated dish at density of 2,000 cells cm^{-2} and 40,000 cells cm^{-2} were cultured for 24 h to obtain sparse and confluent cell cultures, respectively. After starvation in medium 199 containing 1% BSA for 6 h, the cells were stimulated with COMP-Ang1 and growth media (HuMedia-EG2 supplemented with a growth additive set (Kurabo)) as described in the figures. When indicated in the figures, the cells were stimulated in the presence of 20 μM U0126 (Cell Signaling Technology), 20 μM LY294002 (Cell Signaling Technology), or 8 μM Akt inhibitor IV (Calbiochem). Cells washed twice with ice-cold PBS were lysed at 4 °C in RIPA buffer containing 50 mM Tris-HCl at pH7.5, 150 mM NaCl, 1% Triton X-100, 0.5% sodium deoxycholate, 0.1% sodium dodecyl sulfate, 20 mM sodium fluoride, 1 mM sodium vanadate and 1 x protease inhibitor cocktail and centrifuged at 15,000*g* for 20 min at 4 °C. The supernatant was used as precleared cell lysate. To quantify the phosphorylated Tie2, Tie2 was immunoprecipitated with anti-Tie2 antibody from the precleared lysates. Immunoprecipitated Tie2 and aliquots of cell lysate were subjected to SDS-PAGE and Western blot analysis with anti-phosphotyrosine and anti-Tie2 antibodies, respectively. To evaluate the phosphorylation of Erk, Akt, Foxo1 and eNOS, aliquots of total cell lysate were subjected to Western blot analysis with anti-phospho-Erk, anti-phospho-Akt, anti-phospho-Foxo1 and anti-phospho-eNOS antibodies. The total contents of Erk, Akt, Foxo1 and eNOS were also assayed in a parallel run using corresponding antibodies.

To stimulate BaF3 and BaF-Tie2 cells in either floating or adhering condition, the cells were starved for 4 h in RPMI1640 media. The cells were then either allowed to attach to fibronectin-coated dish (attached cells) or kept in 15 ml-conical tube (suspended cells) for 30 min at 37 °C, and stimulated as described in the figures. For the cells

stimulated on fibronectin coated-dish, the supernatants containing floating cells were transferred to 15 ml-conical tubes including ice-cold PBS, collected by centrifugation, and lysed in RIPA buffer. The adhering cells were lysed in RIPA buffer, and both lysates were combined. For the suspended cells, the reactions were stopped by adding ice-cold PBS into the tubes, and the cells were collected by centrifugation and lysed in RIPA buffer. To stimulate floating and adhering HUVECs, the cells starved in 1% BSA for 6 h were detached from the culture dish using Cell dissociation buffer (CDB: Invitrogen Corp.). The cells either allowed to adhere on collagen-coated dish or kept in 15 ml-conical tube for 1 h at 37°C were stimulated with COMP-Ang1 for 15 min. The floating and adhering cells were lysed as described for BaF3 and BaF-Tie2 cells. Phosphorylation of Tie2, Erk, and Akt was analyzed as described above.

Stimulation of HUVECs with ECM-bound COMP-Ang1. To stimulate HUVECs with ECM-bound COMP-Ang1, collagen-coated glass-base dishes were incubated with 3 μg ml^{-1} COMP-Ang1 in PBS for 2 h at 37 °C, and washed four times with PBS. HUVECs starved in medium 199 containing 1% BSA for 3 h were detached from the culture dish using CDB, and resuspended in medium 199 containing 0.5% BSA. The cells were placed on the COMP-Ang1-bound dish and incubated for the periods indicated in the figure. After washing with PBS, the cells were fixed and stained with anti-Tie2, anti-vinculin, anti-FAK antibodies and rhodamine-phalloidin as described above. To quantify the formation of focal complexes, fluorescence intensity relative to vinculin at the cell periphery was measured by line intensity scanning using MetaMorph 6.1 software.

To examine Tie2 activation by ECM-bound COMP-Ang1, 10 cm-collagen dish was incubated with 3 μg ml^{-1} COMP-Ang1 in PBS for 2 h at 37 °C, and washed four times with PBS. HUVECs starved in medium 199 containing 1% BSA for 6 h were detached using CDB, and resuspended in medium 199. The cells were then placed on the COMP-Ang1-bound dish for 20 min, washed twice with ice-cold PBS, and lysed at 4 °C in RIPA buffer. Then, lysates were centrifuged at 15,000 rpm for 20 min at 4 °C. The phosphorylation of Tie2 was examined as described above.

To examine the effects of ECM-bound COMP-Ang1 and MEK inhibitor U0126 on endothelial migration, both lower and upper sides of transwell membrane filters (6.5-

mm diameter, 8.0-μm pore size polycarbonate filter, Corning Coster Corporation, Tokyo, Japan) were coated with 0.3 mg ml^{-1} collagen type I in 1 mM HCl at 4 °C overnight, washed with PBS and air-dried. Subsequently, lower side of the membranes were coated with or without 3 μg ml^{-1} COMP-Ang1 in PBS at 37 °C for 2 h, and washed three times with PBS. Before experiments, HUVECs were starved in medium 199 containing 1% FCS for 48 h, detached from the dish using CDB, and resuspended in medium 199 containing 1% FCS at a density of 3.0×10^5 cells ml^{-1}. The cells were preincubated with or without 20 μM U0126 for 1 h at 37 °C and then seeded into the precoated transwell inserts placed in a 24-well plate containing 600 μl medium 199 containing 1% FCS (3×10^4 cells $well^{-1}$). After 5 h, the upper membrane of the inserts was swabbed to remove nonmigrated cells. Then, the inserts were washed four times with PBS, fixed in 100% methanol for 2 min at -20 °C, and stained with Hoechst 33342 (Sigma-Aldrich). Migration of HUVEC was quantified by counting the number of the cells in six random fields per insert.

Detection of subcellular localization of GFP-Foxo1. Sparse and confluent HUVECs grown on collagen-coated glass-base dish were transfected with a pEGFP-C1-Foxo1 vector encoding GFP-Foxo1. Next day, the cells were starved for 6 h in medium 199 containing 0.5% BSA and stimulated with or without COMP-Ang1 for the time periods as indicated in figure. After the stimulation, the cells were washed with PBS and fixed in 100% methanol for 2 min at -20 °C. Fluorescence images of GFP were recorded with an Olympus IX-81 inverted fluorescence microscope, and the number of cells with nuclear localization of GFP-Foxo1 was counted. At least 100 GFP-positive cells were scored for each treatment, and three independent experiments were carried out.

Real-time reverse transcription-PCR. Confluent and sparse HUVECs on collagen-coated dish were starved in HuMedia-EB2 medium containing 0.5% FCS for 15 h, and stimulated with COMP-Ang1 (200 ng ml^{-1}) for 1 h. After the stimulation, total RNA was purified using RNeasy Mini Kit (Qiagen, Valencia, CA). Quantitative real-time reverse transcription-PCR was carried out using QuantiFast SYBR Green RT-PCR kit (Qiagen) according to the manufacturer's instruction. For each reaction, 100 ng of total RNA was

transcribed for 10 min at 50 °C, followed by a denaturing step at 95 °C for 5 min and 40 cycles of 10 s at 95 °C and 30 s at 60 °C. Fluorescence data were collected and analyzed using Mastercycler ep realplex (Eppendorf, Hamburg, Germany). The specificity of amplification was confirmed by melting curve analysis. The primers used for amplification were as follows: for human *KLF10*, 5'-TTCCGGGAACACCTGATTTTC-3' and 5'-GCAATGTGAGGTTTGGCAGTA-3'; for human *SOCS3*, 5'-TGCGCCTCAAGACCTTCAG-3' and 5'-GAGCTGTCGCGGATCAGAAA-3'; for human *KLF2*, 5'-CTACACCAAGAGTTCGCATCTG-3' and 5'-CCGTGTGCTTTCGGTAGTG-3'; for human *TIS11d*, 5'-TGTGCAAGACAGAGAAATCCC-3' and 5'-GAGTGCCGTCGGAGGAATC-3'; for *Cx40*, 5'-TCCTGGAGGAAGTACACAAGC-3' and 5'-ATCACACCGGAAATCAGCCTG-3'; for *glyceraldehyde-3-phosphate dehydrogenase* (*GAPDH*), 5'-ATGGGGAAGGTGAAGGTCG-3' and 5'-GGGGTCATTGATGGCAACAATA-3'. For normalization, expression of human *GAPDH* was determined in parallel as an endogenous control.

Biotinylation of cell surface Tie2. Confluent HUVECs plated on collagen-coated plates were serum-starved in medium 199 containing 1% BSA for 6 h, and stimulated with COMP-Ang1. After the stimulation, the cells were washed with ice-cold PBS, and incubated with 0.5 mg ml^{-1} of EZ Link Sulfo-NHS-Biotin (Pierce Biotechnology, Rockford, IL) for 60 min at 4 °C. The reaction was quenched by treating the cells with 50 mM NH_4Cl in PBS for 10 min 4 °C. The cells were then lysed in RIPA buffer and centrifuged at 15,000 *g* for 20 min at 4 °C. The supernatant was used as precleared cell lysate. Biotinylated proteins were isolated from the lysate with avidin-immobilized agarose beads (Pierce Biotechnology). Precipitated biotinylated proteins and aliquots of cell lysate were subjected to Western blot analysis with anti-Tie2 antibody.

SUPPLEMENTARY REFERENCES

1. Cho, C. H. *et al.* COMP-Ang1: A designed angiopoietin-1 variant with nonleaky angiogenic activity. *Proc.Natl.Acad.Sci.U.S.A* **101**, 5547-5552 (2004).

2. Sakurai, A. *et al.* MAGI-1 is required for Rap1 activation upon cell-cell contact and for enhancement of vascular endothelial cadherin-mediated cell adhesion. *Mol Biol Cell* **17**, 966-976 (2006).

3. Sawano, A., Takahashi, T., Yamaguchi, S., Aonuma, M., & Shibuya, M. Flt-1 but not KDR/Flk-1 tyrosine kinase is a receptor for placenta growth factor, which is related to vascular endothelial growth factor. *Cell Growth Differ.* **7**, 213-221 (1996).

4. Nagashima, K. *et al.* Adaptor protein Crk is required for ephrin-B1-induced membrane ruffling and focal complex assembly of human aortic endothelial cells. *Mol.Biol.Cell* **13**, 4231-4242 (2002).

5. Zamir, E. *et al.* Dynamics and segregation of cell-matrix adhesions in cultured fibroblasts. *Nat.Cell Biol* **2**, 191-196 (2000).

6. Matsuzaki, H., Daitoku, H., Hatta, M., Tanaka, K., & Fukamizu, A. Insulin-induced phosphorylation of FKHR (Foxo1) targets to proteasomal degradation. *PNAS* **100**, 11285-11290 (2003).

7. Nakae, J., Kitamura, T., Silver, D. L., & Accili, D. The forkhead transcription factor Foxo1 (Fkhr) confers insulin sensitivity onto glucose-6-phosphatase expression. *J.Clin.Invest.* **108**, 1359-1367 (2001).

8. Fukuhara, S. *et al.* Cyclic AMP potentiates vascular endothelial cadherin-mediated cell-cell contact to enhance endothelial barrier function through an Epac-Rap1 signaling pathway. *Mol Cell Biol* **25**, 136-146 (2005).

9. Takakura, N. *et al.* Critical role of the TIE2 endothelial cell receptor in the development of definitive hematopoiesis. *Immunity* **9**, 677-686 (1998).

THE JOURNAL OF BIOLOGICAL CHEMISTRY VOL. 283, NO. 35, pp. 24234–24244, August 29, 2008

Interaction of Scaffolding Adaptor Protein Gab1 with Tyrosine Phosphatase SHP2 Negatively Regulates IGF-I-dependent Myogenic Differentiation via the ERK1/2 Signaling Pathway*[S]

Received for publication, May 21, 2008, and in revised form, June 18, 2008 Published, JBC Papers in Press, June 23, 2008, DOI 10.1074/jbc.M803907200

Tatsuya Koyama[‡§1], Yoshikazu Nakaoka[‡¶1,2], Yasushi Fujio[‖], Hisao Hirota[¶†], Keigo Nishida[**], Shoko Sugiyama[¶], Kitaro Okamoto[¶], Keiko Yamauchi-Takihara[¶], Michihiro Yoshimura[§], Seibu Mochizuki[§], Masatsugu Hori[¶], Toshio Hirano[‡‡], and Naoki Mochizuki[‡]**

From the [‡]Department of Structural Analysis, National Cardiovascular Center Research Institute, 5-7-1, Fujishirodai, Suita, Osaka, 565-8565, the [¶]Department of Cardiovascular Medicine, Osaka University Graduate School of Medicine, 2-2, Yamadaoka, Suita, Osaka, 565-0871, the [‖]Department of Clinical Pharmacology and Pharmacogenomics, Osaka University Graduate School of Pharmaceutical Sciences, 1-6, Yamadaoka, Suita, Osaka, 565-0871, the [**]Laboratory for Cytokine Signaling, RIKEN Research Center for Allergy and Immunology, 1-7-22, Suehiro-cho, Tsurumi-ku, Yokohama City, Kanagawa, 230-0045, the [§]Division of Cardiology, Department of Internal Medicine, The Jikei University School of Medicine, 3-25-8, Nishi-Shinbashi, Minato-ku, Tokyo, 105-8461, and the [‡‡]Laboratory of Developmental Immunology, Osaka University Graduate School of Frontier Biosciences and Graduate School of Medicine, 2-2, Yamadaoka, Suita, Osaka, 565-0871, Japan

Grb2-associated binder 1 (Gab1) coordinates various receptor tyrosine kinase signaling pathways. Although skeletal muscle differentiation is regulated by some growth factors, it remains elusive whether Gab1 coordinates myogenic signals. Here, we examined the molecular mechanism of insulin-like growth factor-I (IGF-I)-mediated myogenic differentiation, focusing on Gab1 and its downstream signaling. Gab1 underwent tyrosine phosphorylation and subsequent complex formation with protein-tyrosine phosphatase SHP2 upon IGF-I stimulation in C2C12 myoblasts. On the other hand, Gab1 constitutively associated with phosphatidylinositol 3-kinase regulatory subunit p85. To delineate the role of Gab1 in IGF-I-dependent signaling, we examined the effect of adenovirus-mediated forced expression of wild-type Gab1 ($Gab1^{WT}$), mutated Gab1 that is unable to bind SHP2 ($Gab1^{\Delta SHP2}$), or mutated Gab1 that is unable to bind p85 ($Gab1^{\Delta p85}$), on the differentiation of C2C12 myoblasts. IGF-I-induced myogenic differentiation was enhanced in myoblasts overexpressing $Gab1^{\Delta SHP2}$, but inhibited in those overexpressing either $Gab1^{WT}$ or $Gab1^{\Delta p85}$. Conversely, IGF-I-induced extracellular signal-regulated kinase 1/2 (ERK1/2) activation was significantly repressed in myoblasts overexpressing $Gab1^{\Delta SHP2}$ but enhanced in those overexpressing either $Gab1^{WT}$ or $Gab1^{\Delta p85}$. Furthermore, small interference RNA-mediated Gab1 knockdown enhanced myogenic differentiation. Overexpression of catalytic-inactive SHP2 modulated IGF-I-induced myogenic differentiation and ERK1/2 activation similarly to that of $Gab1^{\Delta SHP2}$, suggesting that Gab1-SHP2 complex inhibits IGF-I-dependent myogenesis through ERK1/2. Consistently, the blockade of ERK1/2 pathway reversed the inhibitory effect of $Gab1^{WT}$ overexpression on myogenic differentiation, and constitutive activation of the ERK1/2 pathway suppressed the enhanced myogenic differentiation by overexpression of $Gab1^{\Delta SHP2}$. Collectively, these data suggest that the Gab1-SHP2-ERK1/2 signaling pathway comprises an inhibitory axis for IGF-I-dependent myogenic differentiation.

Skeletal muscle differentiation is a multistep process in which multipotent mesodermal cells give rise to myoblasts that subsequently withdraw from the cell cycle and differentiate into multinucleated myotubes. Most skeletal muscle cell lines from rodents proliferate in high serum conditions containing various mitogens, and post-confluent cells spontaneously differentiate after several days in low serum conditions (1, 2). Among various growth factors, the insulin-like growth factors (IGFs),[3] includ-

* This work was supported by grants from the Ministry of Education, Science, Sports and Culture of Japan (to Y. N., K. Y.-T., and N. M.); the Ministry of Health, Labour, and Welfare of Japan (to N. M.); the Program for the Promotion of Fundamental Studies in Health Sciences of the National Institute of Biomedical Innovation (to N. M.); the Takeda Medical Research Foundation (to N. M.); The Uehara Memorial Foundation (to Y. N.); the Japan Heart Foundation Young Investigator's Research Grant (to Y. N.); the Suzuken Memorial Foundation (to Y. N.); the Astellas Foundation for Research on Metabolic Disorders (to Y. N.); the Senri Life Science Foundation (to Y. N.); and the Miyata Cardiology Research Promotion Funds (to Y. N.). The costs of publication of this article were defrayed in part by the payment of page charges. This article must therefore be hereby marked "*advertisement*" in accordance with 18 U.S.C. Section 1734 solely to indicate this fact.

[S] The on-line version of this article (available at http://www.jbc.org) contains supplemental text, references, and Figs. S1 and S2.

† Deceased on December 27, 2005.

1 Both authors contributed equally to this work.

2 To whom correspondence should be addressed: Dept. of Cardiovascular Medicine, Osaka University Graduate School of Medicine, Suita, Osaka 565-0871, Japan. Tel.: 81-6-6879-3835; Fax: 81-6-6879-3839; E-mail: ynakaoka@imed3.med.osaka-u.ac.jp.

3 The abbreviations used are: IGF, insulin-like growth factor; Gab1, Grb2-associated binder 1; Gab2, Grb2-associated binder 2; WT, wild-type; PI3K, phosphatidylinositol 3-kinase; MAPK, mitogen-activated protein kinase; MEK1/2, MAPK/extracellular signal-regulated kinase kinase 1/2; ERK1/2, extracellular signal-regulated kinase 1/2; SH2, Src homology 2; SHP2, SH2-containing protein-tyrosine phosphatase 2; EGF, epidermal growth factor; VEGF, vascular endothelial growth factor; IRS-1, insulin receptor substrate-1; MHC, myosin heavy chain; DMEM, Dulbecco's modified Eagle's medium; FBS, fetal bovine serum; β-gal, β-galactosidase; HS, horse serum; FGF2, fibroblast growth factor 2; IP, immunoprecipitation; ANOVA, analysis of variance; siRNA, small interference RNA; RNAi, RNA interference.

ing IGF-I and IGF-II, have been reported to be quite unique in that they stimulate both proliferation and differentiation of muscle cells in culture (3, 4). IGF-I receptor belongs to the receptor tyrosine kinase family and utilizes two major cytoplasmic signaling pathways, namely the phosphatidylinositol 3-kinase (PI3K) cascade and mitogen-activated protein kinase (MAPK) cascade, which consists of Raf-MAPK/extracellular signal-regulated kinase (ERK)-kinase1/2 (MEK1/2)-ERK1/2 (5). PI3K is one of the primary signaling molecules promoting skeletal muscle differentiation, as demonstrated by pharmacological and genetic methods (3, 6, 7). On the other hand, activation of Raf-MEK1/2-ERK1/2 MAPK cascade has been reported to have inhibitory effects on the myogenic differentiation induced by insulin or IGFs (3, 8–10).

Grb2-associated binder 1 (Gab1) belongs to the scaffolding adaptor protein family. Gab1 has an N-terminal pleckstrin homology domain, as well as multiple tyrosine-based motifs and proline-rich sequences, which are potential binding sites for various Src homology 2 (SH2) domains and Src homology 3 domains, respectively. Gab1 undergoes tyrosine phosphorylation upon stimulation with various growth factors, cytokines, G protein-coupled receptor agonists, and various immuno-antigens (11,12). Tyrosine-phosphorylated Gab1 provides docking sites for multiple SH2 domain-containing signaling molecules, such as SH2-containing protein-tyrosine phosphatase SHP2, PI3K regulatory subunit p85, phospholipase C-γ, Crk, and Ras GTPase-activating protein (11–17). Among these binding partners, SHP2, a ubiquitously expressed protein-tyrosine phosphatase, has crucial roles for receptor tyrosine kinase-dependent activation of ERK1/2 in association with Gab1 (18, 19). The functional significance of Gab1-SHP2 interaction has been extensively studied using the Gab1 mutant that is unable to bind SHP2. This Gab1 mutant is defective in delivering signals for hepatocyte growth factor-c-Met-dependent morphogenesis, epidermal growth factor (EGF)-dependent epidermal proliferation, and leukemia inhibitory factor-gp130-dependent cardiomyocyte hypertrophy (20–23). These findings underscore the importance of Gab1-SHP2 interaction and strongly suggest that the primary role of Gab1 might be to recruit SHP2 (24). On the other hand, it has been reported that Gab1 also regulates the PI3K-AKT signaling pathway through association with p85 downstream of various growth factors (25–29). Gab1 has been reported to be required for both EGF-dependent activation of PI3K-AKT signaling pathway and migration of keratinocytes (28–30). In addition, Gab1 plays a key role for vascular endothelial growth factor-dependent activation of the PI3K signaling pathway and is required for endothelial cell migration and capillary formation (25, 27).

Gab1knockout (Gab1KO) mice died *in utero* and displayed developmental defects in the heart, placenta, liver, skin, and skeletal muscle (31, 32). Furthermore, Gab1KO mice displayed reduced and delayed migration of muscle progenitor cells into the limbs and diaphragm, resulting in the immature formation of limb muscles. These data suggest that Gab1 might have a key role in skeletal muscle development (32). We created cardiomyocyte-specific Gab1/Gab2 double knock-out mice and revealed that Gab1 and Gab2 play redundant, but essential roles in postnatal maintenance of cardiac function via the neuregulin-1/ErbB signaling pathway (33). In addition, liver-specific Gab1 knock-out mice displayed enhanced hepatic insulin sensitivity with reduced glycemia and improved glucose tolerance as a result of insufficient insulin-elicited activation of ERK1/2 (34). However, it remains elusive whether Gab1 has a specific role in skeletal muscle differentiation. In this study, we demonstrate for the first time that Gab1-SHP2 interaction exerts an inhibitory effect on IGF-I-induced myogenic differentiation via activation of the ERK1/2 signaling pathway.

EXPERIMENTAL PROCEDURES

Reagents and Antibodies—Anti-phospho-p44/42 ERK1/2 (Thr-202/Tyr-204), anti-phospho-AKT (Thr-308), anti-ERK1/2, and anti-AKT antibodies were purchased from Cell Signaling Technology. Anti-Gab1 and anti-Gab2 sera for immunoprecipitation were described previously (15, 16, 22). The antibodies against the following molecules used for immunoblotting, Gab1, Gab2, insulin receptor substrate-1 (IRS-1), and p85 PI3K were from Millipore; PY99, SHP2, MEK1, and myogenin were from Santa Cruz Biotechnology. Anti-myosin heavy chain (MHC) monoclonal antibody (MF20) was purchased from the Developmental Hybridoma Bank (Dr. D. A. Fischman, University of Iowa, Iowa City, IA). Hoechst 33342 nuclear dye was from Sigma. Horseradish peroxidase-conjugated anti-mouse and anti-rabbit antibodies were from GE Health Science. U0126 was from Promega (Madison, WI). Serum and cell culture reagents were from Invitrogen. Human recombinant IGF-I was kindly provided by Astellas Pharmaceuticals.

Adenovirus Vector Construction—The generation of adenovirus vectors expressing human $Gab1^{WT}$ and $Gab1^{\Delta SHP2}$ (mutated on the two tyrosine residues responsible for binding with SHP2) were described previously (22). In this study, we constructed the adenovirus vectors expressing $Gab1^{\Delta p85}$, which can't bind with p85 due to the substitution of tyrosine residues 447, 472, and 589 of human Gab1, corresponding to the *YXXM* motifs, to phenylalanines by PCR-based mutagenesis described previously (35). Substitution of these tyrosine residues by phenylalanine renders the molecule incapable of binding with p85. We also constructed adenovirus vectors expressing wild-type SHP2 ($SHP2^{WT}$) and phosphatase-inactive SHP2 ($SHP2^{C/S}$) using the plasmid vectors described previously (15). For adenovirus production, the sequence encoding $Gab1^{\Delta p85}$, $SHP2^{WT}$, or $SHP2^{C/S}$ was subcloned into the shuttle plasmid pACCMVpLpA. Recombinant adenoviruses were then obtained according to the homologous recombination system described elsewhere (36). The adenovirus vectors expressing constitutive-active MEK1 and dominant-negative MEK1 were kindly provided by Dr. S. Kawashima (Kobe University) and described previously (37). The construction of adenovirus vector expressing human $Gab2^{\Delta SHP2}$, which can't bind with SHP2, is described in the supplemental data.

Cell Culture, Stimulation, and Adenoviral Infection—C2C12 murine myoblast cells were maintained as subconfluent monolayers in Dulbecco's modified Eagle's medium (DMEM) containing 4.5 g/liter glucose, 0.58 g/liter L-glutamine, 100 units/ml penicillin, and 100 μg/ml streptomycin supplemented with

20% fetal bovine serum (FBS). Before stimulation, cells were serum-starved overnight. Stimulations were performed using 80 ng/ml IGF-I for 10 min, unless otherwise indicated. For adenoviral infection of C2C12 myoblasts, subconfluent cells were cultured in DMEM with 20% FBS at a multiplicity of infection of 50 for 24 h. In the dual infection of adenovirus vectors, C2C12 cells were cultured in DMEM with 20% FBS with each virus at a multiplicity of infection of 30. Then, the myoblasts were serum-starved overnight and stimulated with or without IGF-I for the experiments examining ERK1/2 and AKT phosphorylation. Infection efficiency, determined by *lacZ* gene expression in cultured myoblasts, is consistently >90% with this method. Adenovirus vector expressing β-galactosidase (β-gal) was used as a control. For the induction of myogenic differentiation, cultured medium was switched from DMEM containing 20% FBS to DMEM containing 2% horse serum (HS) or 80 ng/ml IGF-I, when cell density reached confluency. The differentiation medium containing 2% HS was exchanged every other day, and that containing IGF-I was exchanged every day.

Cell Lysis, Immunoprecipitations, and Immunoblotting—Cells were scraped off in lysis buffer containing 20 mM Tris (pH 7.4), 150 mM NaCl, 3 mM EDTA, 1% Nonidet P-40, 2 mM sodium orthovanadate, and protease inhibitor mixture Complete (Roche Applied Science). Cell lysates were collected form confluent 6-cm dishes and precleared by 15,000 × *g* centrifugation for 15 min. For immunoprecipitation, the cleared lysates of 500 μl containing 1 mg of protein, were rotationally incubated with 1 μl of anti-Gab1 antiserum, or 1.2 μg of SHP2 antibody, or 5 μl of p85 antibody, or 10 μl of IRS-1 antibody and with 20 μl of protein A-Sepharose (GE Healthcare) overnight at 4 °C. The antigen-antibody complexes were collected by centrifugation, washed three times with lysis buffer without protease inhibitor mixture, and boiled in standard electrophoresis sample buffer. All the proteins immunoprecipitated were then resolved by SDS-PAGE and subjected to immunoblotting using a standard procedure. Blots were developed using ECL system (GE Healthcare). For direct immunoblotting analyses, the crude cell lysates were collected from 3.5-cm dishes and subjected to 15,000 × *g* centrifugation. The precleared lysates containing 30 μg of protein were loaded in each lane for immunoblotting.

Immunocytochemistry—Cells cultured on 3.5-cm collagen type I-coated plastic dishes (Iwaki Asahi Glass Co.) were fixed with 2% formaldehyde in phosphate-buffered saline and permeabilized with 0.1% Triton X-100 for 10 min. Cells were blocked with phosphate-buffered saline containing 1% bovine serum albumin for 1 h and incubated with anti-MHC antibody (MF20), followed by incubation with Alexa 488-labeled goat anti-mouse secondary antibody (Molecular Probes). Cells were post-stained with Hoechst 33342 nuclear dye and viewed by fluorescence microscopy.

siRNA-mediated Protein Knockdown—Stealth Select small interfering RNAs (siRNAs) targeted to murine Gab1 (#1, MSS204497; #2, MSS204499) and siRNA duplex with irrelevant sequences (Stealth™ RNAi negative control) as a control were purchased from Invitrogen. Stealth siRNAs targeted to murine SHP2 were purchased from Invitrogen. and the detailed sequences are described in the supplemental data. C2C12 myoblasts were transfected with 10 nM siRNA duplexes using Lipofectamine™ RNAiMAX reagent according to the manufacturer's instructions for reverse transfection. Briefly, C2C12 myoblasts (1.5×10^5 cells per each dish) were diluted in 860 μl of DMEM containing 20% FBS and plated on 3.5-cm collagen type I-coated plastic dishes. To each dish, 140 μl of RNAi duplex-Lipofectamine™ RNAiMAX complex diluted in Opti-MEM I medium was added. After incubation for 72 h, the cells were used for the experiments.

Statistics—All data are expressed as mean ± S.D. Differences among multiple groups were compared by one-way ANOVA followed by a post hoc comparison tested with Scheffe's method. Values of $p < 0.05$ were considered significant.

RESULTS

Gab1 Undergoes Tyrosine Phosphorylation and Subsequently Associates with SHP2 upon IGF-I Stimulation in C2C12 Myoblasts—We examined the effect of IGF-I on tyrosine-phosphorylation of Gab1 and its association with SH2 domain-containing signaling molecules in C2C12 myoblasts. IGF-I indeed induced tyrosine phosphorylation of Gab1 and subsequent association of Gab1 with SHP2 in C2C12 myoblasts (Fig. 1*A*, *left panel*). Furthermore, SHP2 was also tyrosine-phosphorylated and associated with Gab1 after stimulation with IGF-I (Fig. 1*A*, *right panel*). On the other hand, Gab1 constitutively associated with p85 both before and after IGF-I stimulation (Fig. 1*A*, *left panel*). In the IGF-I-dependent signaling pathway, IRS-1 has been reported to be a major binding partner of p85 and essential for IGF-I-dependent PI3K-AKT signaling in skeletal muscle cells (38). Consistently, IRS-1 underwent strong tyrosine phosphorylation after stimulation with IGF-I in C2C12 myoblasts. In clear contrast to Gab1, IRS-1 associated with p85 in a manner dependent on IGF-I stimulation (Fig. 1*B*). In addition, we could not detect the complex formation of IRS-1 with SHP2 either before or after stimulation with IGF-I (Fig. 1*B*). These results demonstrate that IGF-I induces tyrosine phosphorylation of Gab1, leading to complex formation of Gab1 with SHP2 in C2C12 myoblasts.

IGF-I-induced Tyrosine Phosphorylation of Gab1 and Association of Gab1 with SH2 Domain-containing Molecules in the C2C12 Myoblasts Infected with Adenovirus Vectors—IGFs have been reported to stimulate both proliferation and differentiation of cultured skeletal muscle cells (3, 4). The effect of IGF-I on the proliferation of myoblasts has been reported to be attributed mainly to ERK1/2 pathway (3). In the present study, we tried to reveal the role of Gab1 in IGF-I-dependent differentiation from myoblasts into myotubes. To discern the role of Gab1-SHP2 interaction from that of Gab1-p85 interaction in IGF-I-dependent differentiation, we used recombinant adenovirus vectors carrying β-gal (control), $Gab1^{WT}$, or $Gab1^{\Delta SHP2}$ as described previously (22) and created an adenovirus vector overexpressing $Gab1^{\Delta p85}$. We examined tyrosine phosphorylation of Gab1 upon stimulation with IGF-I in myoblasts overexpressing β-gal, $Gab1^{WT}$, $Gab1^{\Delta SHP2}$, or $Gab1^{\Delta p85}$. As shown in Fig. 2*A*, tyrosine phosphorylation of Gab1 and the amount of co-immunoprecipitated SHP2 with Gab1 were increased after stimulation with IGF-I in control myoblasts expressing β-gal. On the other hand, tyrosine phosphorylation of Gab1 in the

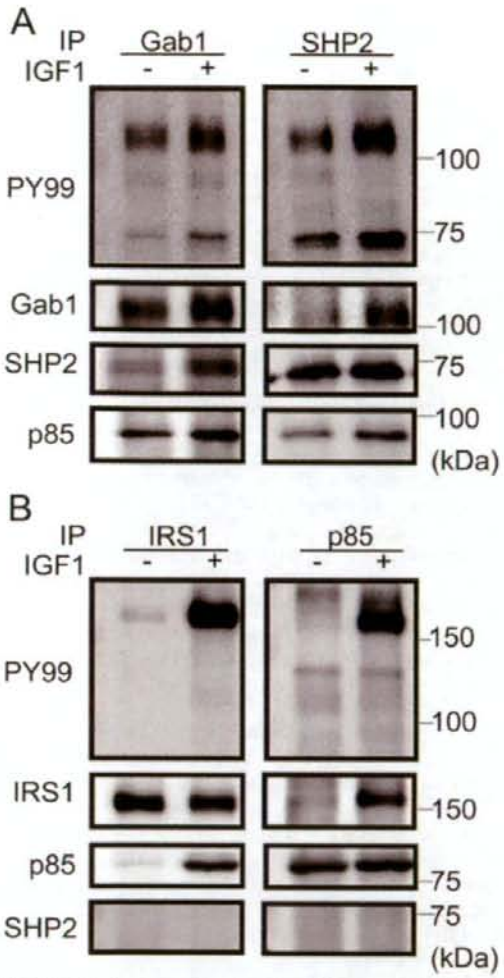

FIGURE 1. **IGF-I induces tyrosine phosphorylation of Gab1 and complex formation of Gab1 with SHP2 in C2C12 myoblasts.** Serum-starved C2C12 myoblast cells were stimulated with 80 ng/ml IGF-I for 10 min, and cell lysates of 500 μl harvested from 6 cm dishes were subjected to immunoprecipitation analysis with anti-Gab1 serum (*A, left panel*), anti-SHP2 antibody (*A, right panel*), anti-IRS-1 antibody (*B, left panel*), or anti-p85 antibody (*B, right panel*). Immunoprecipitates were subjected to SDS-PAGE followed by immunoblot analysis with anti-phosphotyrosine antibody (PY99). The same membrane was reprobed with the antibodies indicated at the *left* (anti-Gab1, anti-SHP2, and anti-p85 antibodies). *A*, both Gab1 and SHP2 were tyrosine-phosphorylated and co-immunoprecipitated with each other in an IGF-I-dependent manner. On the other hand, the association of Gab1 with p85 did not change either before or after IGF-I treatment. *B*, upon stimulation with IGF-I, IRS-1 became strongly tyrosine-phosphorylated and co-immunoprecipitated with p85. However, co-immunoprecipitation of IRS-1 with SHP2 was not detected. Experiments were repeated three times with similar results.

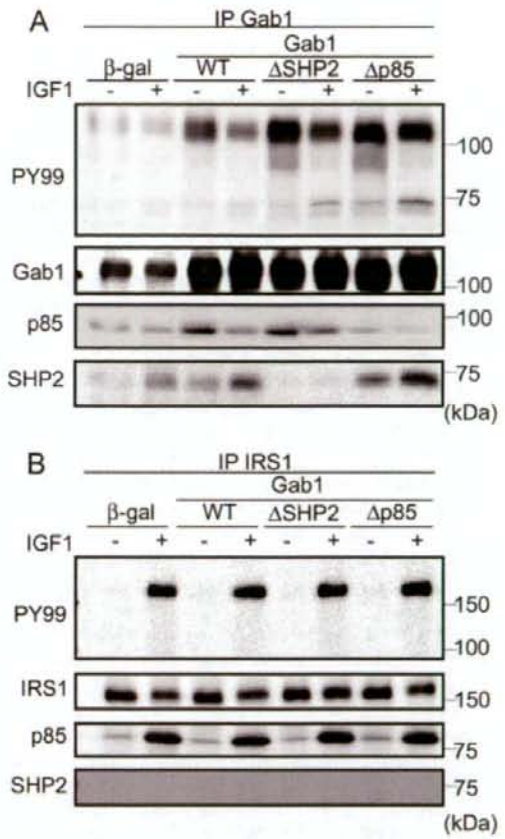

FIGURE 2. **Overexpression of Gab1$^{\Delta SHP2}$ or Gab1$^{\Delta p85}$ specifically perturbs the IGF-I-dependent molecular association of Gab1 with SHP2 or p85, respectively.** C2C12 myoblasts were infected with adenovirus vectors expressing β-gal, Gab1^{WT}, Gab1$^{\Delta SHP2}$, or Gab1$^{\Delta p85}$. Serum-starved C2C12 cells were stimulated with vehicle (−) or IGF-I for 10 min, and cell lysates of 500 μl were collected from 6-cm dishes. Cell lysates were subjected to immunoprecipitation with anti-Gab1 serum (*A*) or with anti-IRS-1 antibody (*B*), followed by immunoblotting with anti-phosphotyrosine antibody (PY99). *A*, blots were reprobed with anti-Gab1, anti-p85, and anti-SHP2 antibodies. *B*, blots were reprobed with anti-IRS-1, anti-p85, and anti-SHP2 antibodies. Experiments were repeated three times with similar results.

myoblasts overexpressing Gab1^{WT}, Gab1$^{\Delta SHP2}$, or Gab1$^{\Delta p85}$ increased much more at baseline compared with in those overexpressing β-gal. In these cells, tyrosine phosphorylation of Gab1 decreased after stimulation with IGF-I. The IGF-I-induced association of Gab1 with SHP2 increased in the C2C12 myoblasts overexpressing Gab1^{WT}, or Gab1$^{\Delta p85}$ compared with those overexpressing β-gal, but was almost abrogated in those overexpressing Gab1$^{\Delta SHP2}$ (Fig. 2*A*). The co-immunoprecipitation of Gab1 with p85 was increased in cells expressing Gab1^{WT} or Gab1$^{\Delta SHP2}$ compared with those expressing β-gal, but was almost abrogated in those expressing Gab1$^{\Delta p85}$ at the baseline. The association of Gab1 with p85 decreased in response to IGF-I in the cells overexpressing Gab1^{WT} or Gab1$^{\Delta SHP2}$ (Fig. 2*A*). We observed much more dissociation of p85 from Gab1 in myoblasts overexpressing Gab1^{WT} compared with those overexpressing Gab1$^{\Delta SHP2}$, which might be attributed to the increased activation of SHP2. Presumably, SHP2 dephosphorylates the tyrosine residues for p85 binding site of Gab1 consistent with the previous report on EGF-dependent signaling (39). These data demonstrate that overexpression of

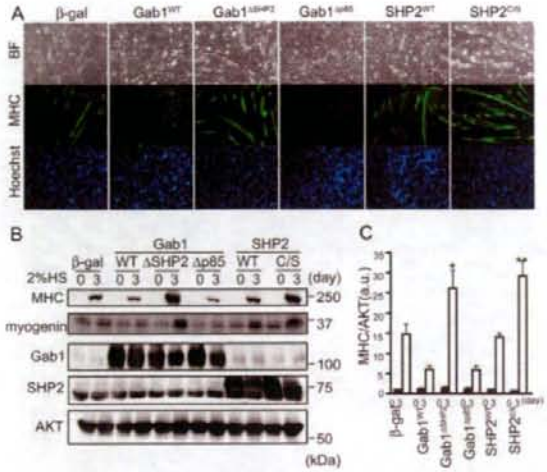

FIGURE 3. **Myogenic differentiation in a low serum condition is negatively regulated by Gab1-SHP2 complex through activating phosphatase activity of SHP2 in C2C12 myoblasts.** *A*, immunocytochemical analysis of C2C12 myoblasts using anti-MHC antibody. C2C12 myoblasts were infected with adenovirus vectors expressing β-galactosidase (β-gal), $Gab1^{WT}$, $Gab1^{\Delta SHP2}$, $Gab1^{\Delta p85}$, $SHP2^{WT}$, or $SHP2^{C/S}$ and induced into myogenic differentiation by switching the growth medium containing 20% fetal bovine serum to the differentiation medium containing 2% horse serum. On the third day after induction, cells were immunostained with anti-MHC antibody and post-stained with nuclear dye Hoechst 33342. *BF*, bright field image. Experiments were repeated three times with similar results. *B*, Western blot analysis of myoblasts infected with indicated adenovirus vectors before and after low serum-induced myogenic induction for 3 days. Cell lysates were subjected to Western blot analysis using anti-MHC and anti-myogenin antibodies. The membrane was stripped and reprobed with anti-Gab1 or anti-SHP2 antibodies for confirmation of adenoviral overexpression of Gab1 or SHP2. AKT expression was also examined for loading control. *C*, the relative expression level of MHC was quantified by normalizing the expression of MHC by that of AKT. Values are expressed as means ± S.D. of three independent experiments (*, $p < 0.05$ or **, $p < 0.01$ compared with control cells expressing β-gal on the same day after myogenic induction, by one-way ANOVA). *a.u.*, arbitrary unit(s).

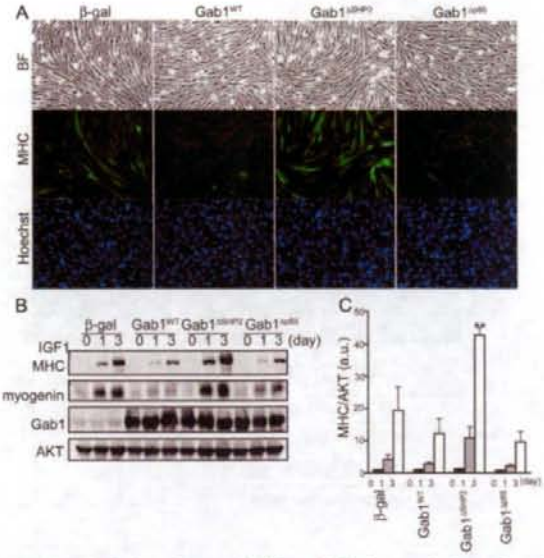

FIGURE 4. **IGF-I-induced myogenic differentiation is negatively regulated by interaction of Gab1 with SHP2 in C2C12 myoblasts.** *A*, immunocytochemical analysis of C2C12 myoblasts overexpressing various Gab1 proteins. C2C12 myoblasts infected with adenovirus vectors overexpressing β-gal, $Gab1^{WT}$, $Gab1^{\Delta SHP2}$, or $Gab1^{\Delta p85}$ (as indicated at the top), were cultured in differentiation medium containing IGF-I. On the third day after exposure to the differentiation medium containing IGF-I, cells were immunostained with anti-MHC antibody and post-stained with Hoechst 33342 nuclear dye. Experiments were repeated three times with similar results. *B*, cell lysates were collected from C2C12 cells overexpressing β-gal, $Gab1^{WT}$, $Gab1^{\Delta SHP2}$, or $Gab1^{\Delta p85}$ at the indicated time after cultivation in the differentiation medium containing IGF-I. Cell lysates were subjected to Western blot analysis for analyzing the expression of MHC and myogenin. The membrane was reprobed with anti-Gab1 antibody for confirmation of adenoviral overexpression of Gab1. AKT was also examined as a loading control. *C*, the relative expression level of MHC was quantified by normalizing the expression of MHC by that of AKT. Values are shown as mean ± S.D. of three independent experiments (**, $p < 0.01$ compared with control cells expressing β-gal on the same day after myogenic induction, by one-way ANOVA). *a.u.*, arbitrary unit(s).

$Gab1^{\Delta SHP2}$ or $Gab1^{\Delta p85}$ sufficiently suppresses the association of Gab1 with SHP2 or p85, respectively.

On the other hand, tyrosine phosphorylation of IRS-1 and interaction between IRS-1 and p85 were comparable among the four groups of cells after stimulation with IGF-I (Fig. 2*B*). Thus, these findings indicate that overexpression of $Gab1^{\Delta SHP2}$ or $Gab1^{\Delta p85}$ specifically perturbs the IGF-I-dependent interaction of Gab1 with SHP2 or p85, respectively.

Myogenic Differentiation Induced by a Low Serum Condition Is Negatively Regulated by Gab1-SHP2 Complex through Activating SHP2 in C2C12 Myoblasts—C2C12 myoblasts undergo myogenic differentiation under a low-serum condition such as 2% HS (1, 2). Therefore, we examined the effects of overexpression of $Gab1^{WT}$, $Gab1^{\Delta SHP2}$, or $Gab1^{\Delta p85}$, on myogenic differentiation under low serum condition. After infection with adenovirus vectors for 24 h, confluent C2C12 myoblasts were cultured in the DMEM containing 2% HS. On the third day after induction of myogenic differentiation, cells were immunostained with anti-MHC antibody for evaluation of myogenic differentiation. The extent of myogenic differentiation was enhanced in myoblasts overexpressing $Gab1^{\Delta SHP2}$, but inhibited in myoblasts overexpressing either $Gab1^{WT}$ or $Gab1^{\Delta p85}$, compared with myoblasts infected with control adenovirus vector expressing β-gal (Fig. 3*A*). Western blot analysis also revealed that the expression of MHC was significantly increased by the overexpression of $Gab1^{\Delta SHP2}$, but seemed to be repressed by the overexpression either $Gab1^{WT}$ or $Gab1^{\Delta p85}$, compared with control (Fig. 3, *B* and *C*). These findings indicate that Gab1-SHP2 interaction exerts an inhibitory effect on myogenic differentiation induced by a low serum condition.

Gab1-SHP2 complex formation has been reported to result in an increase of phosphatase activity of SHP2 upon stimulation with EGF (20, 21, 24). To confirm the requirement of catalytic activity of SHP2 for inhibition of myogenesis, we created adenovirus vectors expressing wild-type SHP2 ($SHP2^{WT}$) and phosphatase-inactive SHP2 ($SHP2^{C/S}$). After infection with adenovirus vectors for 24 h, confluent C2C12 myoblasts were cultured in the DMEM containing 2% HS. The extent of myogenic differentiation determined by immunocytochemistry was enhanced in myoblasts overexpressing $SHP2^{C/S}$ compared with myoblasts overexpressing β-gal or $SHP2^{WT}$ (Fig. 3*A*). Consistently, Western blot analysis showed that overexpression of $SHP2^{C/S}$ in C2C12 cells induced significant increase of MHC

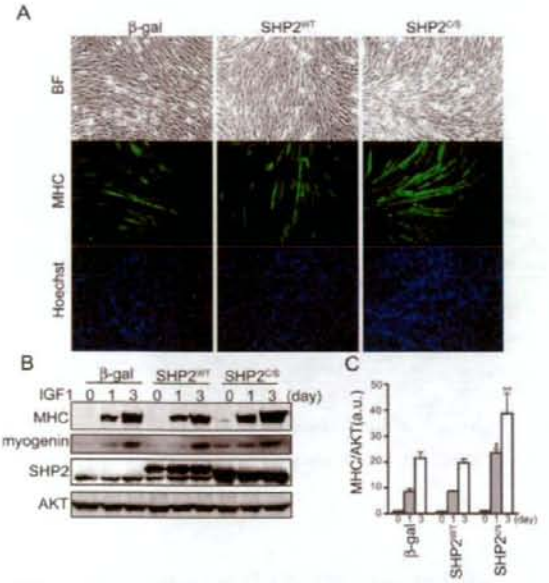

FIGURE 5. **SHP2 phosphatase activity is required for inhibition of myogenic differentiation.** *A*, C2C12 myoblasts overexpressing β-gal, $SHP2^{WT}$, or $SHP2^{C/S}$ were cultured in differentiation medium containing IGF-I. On the third day after exposure to the differentiation medium, cells were immunostained with anti-MHC antibody and post-stained with Hoechst 33342 nuclear dye. Myogenic differentiation was enhanced in myoblasts overexpressing $SHP2^{C/S}$ compared with myoblasts overexpressing β-gal and $SHP2^{WT}$. Experiments were repeated three times with similar results. *B*, cell lysates were collected from C2C12 cells overexpressing β-gal, $SHP2^{WT}$, or $SHP2^{C/S}$ at the indicated time after cultivation in the differentiation medium containing IGF-I. Cell lysates were subjected to Western blot analysis for analyzing the expression of MHC and myogenin. The membrane was reprobed with anti-SHP2 antibody for confirmation of adenoviral overexpression of SHP2. AKT was examined as a loading control. *C*, the relative expression level of MHC was quantified by normalizing the expression of MHC by that of AKT. Values are shown as means ± S.D. (*, $p < 0.05$ or **, $p < 0.01$ compared with control cells expressing β-gal on the same day after myogenic induction, by one-way ANOVA). *a.u.*, arbitrary unit(s).

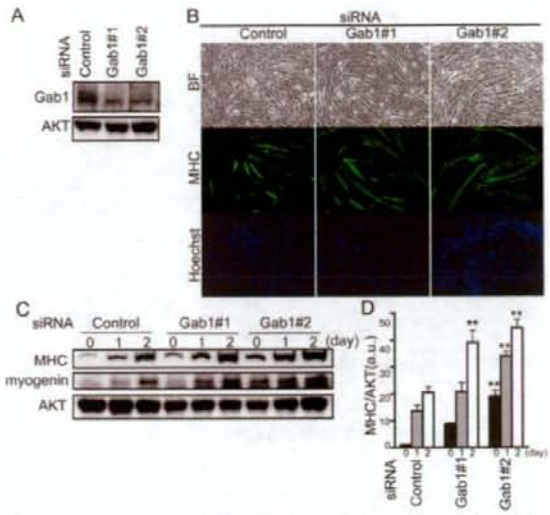

FIGURE 6. **siRNA-mediated Gab1 knockdown enhances myogenic differentiation.** *A*, C2C12 myoblasts were transfected with control siRNA (control) or with two independent siRNAs targeting different sequences of Gab1 (Gab1#1 and Gab1#2) for 72 h. Cell lysates were subjected to Western blot analysis. AKT was also checked as a loading control. *B*, C2C12 myoblasts were transfected with siRNAs as described in Fig. 6*A*. On the third day after transfection, the medium was changed from growth medium containing 20% FBS to differentiation medium containing 80 ng/ml IGF-I. Cells were cultured in the presence of IGF-I for 2 days. Cells were immunostained with anti-MHC antibody and post-stained with Hoechst 33342 nuclear dye. Experiments were repeated three times with similar results. *C*, cell lysates were collected at the indicated time after induction of myogenic differentiation and subjected to Western blot analysis. On the first and second day after myogenic induction, the expression level of MHC and myogenin were increased in cells transfected with Gab1 siRNAs (#1 or #2) compared with control. AKT was examined as a loading control. *D*, the relative expression level of MHC was quantified by normalizing the expression of MHC by that of AKT. Values are shown as means ± S.D. (**, $p < 0.01$ compared with control cells on the same day after myogenic induction, by one-way ANOVA). *a.u.*, arbitrary unit(s).

expression, compared with control (Fig. 3, *B* and *C*). Taken together, these findings suggest that Gab1 exerts an inhibitory effect on myogenic differentiation of C2C12 myoblasts under low serum condition through association with SHP2 and increase of SHP2 catalytic activity.

IGF-I-induced Myogenic Differentiation Is Negatively Regulated by Gab1-SHP2 Complex through Increasing Catalytic Activity of SHP2 in C2C12 Myoblasts—The IGF family, including IGF-I and -II, induces myogenic differentiation of myoblasts after myoblasts fully proliferate and become ready for differentiation (1–3). Therefore, we examined the effect of overexpression of various Gab1 proteins on the myogenic differentiation of C2C12 myoblasts cultured in IGF-I-containing differentiation medium. After infection with adenovirus vectors for 24 h, post-confluent C2C12 myoblasts were cultured in the DMEM containing 80 ng/ml IGF-I. On the third day after induction of myogenic differentiation, cells were immunostained with anti-MHC antibody. The extent of myogenic differentiation was enhanced in myoblasts overexpressing $Gab1^{\Delta SHP2}$ but inhibited in myoblasts overexpressing $Gab1^{WT}$ or $Gab1^{\Delta p85}$, compared with control (Fig. 4*A*). MHC expression was significantly increased in the myoblasts overexpressing $Gab1^{\Delta SHP2}$, although it seemed to be repressed in those overexpressing $Gab1^{WT}$ or $Gab1^{\Delta p85}$, compared with control (Fig. 4, *B* and *C*). Furthermore, the expression of myogenin was enhanced in myoblasts overexpressing $Gab1^{\Delta SHP2}$, but repressed in myoblasts overexpressing $Gab1^{WT}$ or $Gab1^{\Delta p85}$, compared with control (Fig. 4*B*). These data coincide with the results observed in the low serum condition, suggesting that Gab1-SHP2 complex has an inhibitory role in the IGF-I-induced myogenic differentiation.

Gab2, another Gab family protein, has been reported to complement the function of Gab1 in some signaling pathways such as EGF-dependent signaling (33, 40). To confirm the specific role of Gab1 in myogenic differentiation, we examined the effect of overexpression of $Gab2^{\Delta SHP2}$, the Gab2 mutant that cannot associate with SHP2 (41), on IGF-I-induced myogenic differentiation. The extent of myogenic differentiation was comparable between myoblasts overexpressing $Gab2^{\Delta SHP2}$ and those expressing β-gal (supplemental Fig. S1, *A* and *B*). We also confirmed that $Gab2^{\Delta SHP2}$ did not associate with SHP2 either before or after stimulation with IGF-I (supplemental Fig. S1*C*). These data suggested that IGF-I-induced myogenic differenti-

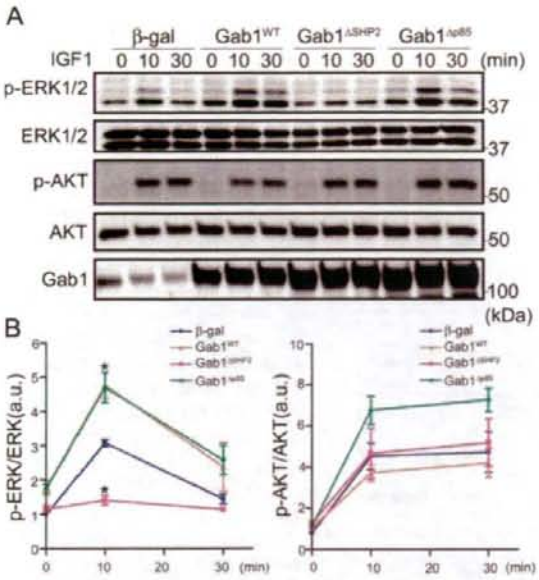

FIGURE 7. **IGF-I activates ERK1/2 via complex formation of Gab1 with SHP2 in C2C12 cells.** *A*, C2C12 cells infected with the indicated adenovirus vectors were serum-starved overnight and stimulated with IGF-I (80 ng/ml) for the indicated period. Cell lysates were collected at the indicated time and subjected to Western blot analysis using the antibodies indicated at the left. Expression level of Gab1 was almost comparable in the cells overexpressing $Gab1^{WT}$, $Gab1^{\Delta SHP2}$, or $Gab1^{\Delta p85}$. *B*, phosphorylation of ERK1/2 (*left*) and AKT (*right*) in *A* was quantified. Values are expressed as means ± S.D. of three independent experiments (*, $p < 0.05$, compared with control cells expressing β-gal at the same time after stimulation, by one-way ANOVA). *a.u.*, arbitrary unit(s).

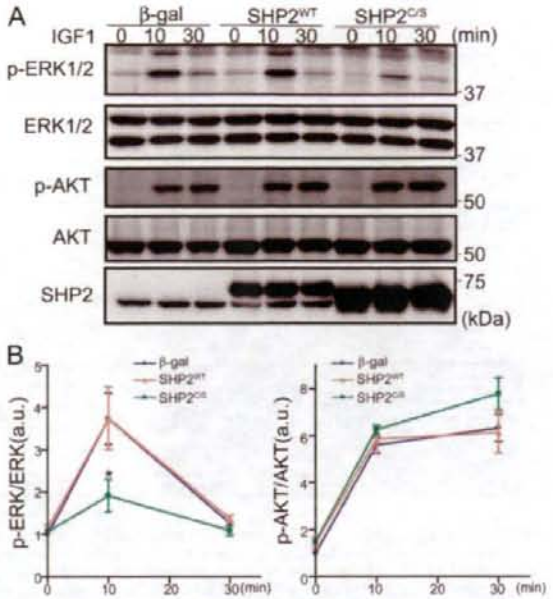

FIGURE 8. **IGF-I activates ERK1/2 via activation of SHP2 in C2C12 cells.** *A*, C2C12 cells infected with indicated adenovirus vectors were treated the same as in Fig. 7. Cell lysates were collected and subjected to Western blot analysis for analyzing ERK1/2 and AKT phosphorylation using the antibodies indicated at the left. Adenovirus-mediated overexpression of SHP2 was almost comparable in cells expressing $SHP2^{WT}$ or $SHP2^{C/S}$. *B*, phosphorylation of ERK1/2 (*left*) and AKT (*right*) in *A* was quantified. Values are shown as means ± S.D. from three independent experiments (*, $p < 0.05$ compared with control cells expressing β-gal at the same time after IGF-I stimulation, by one-way ANOVA). *a.u.*, arbitrary unit(s).

ation in C2C12 myoblasts might be regulated specifically by Gab1-SHP2 complex, but not by Gab2-SHP2 complex.

To confirm the requirement of SHP2 catalytic activity for the inhibitory effect of Gab1-SHP2 complex on myogenesis, C2C12 myoblasts were infected with adenovirus vectors expressing β-gal, $SHP2^{WT}$, or $SHP2^{C/S}$ and then treated with IGF-I-containing differentiation medium for the induction of myogenesis. Myogenic differentiation was enhanced in myoblasts overexpressing $SHP2^{C/S}$ compared with myoblasts overexpressing β-gal or $SHP2^{WT}$ (Fig. 5*A*). Western blot analysis also demonstrated that the MHC expression was significantly increased in the myoblasts overexpressing $SHP2^{C/S}$, but not in those overexpressing $SHP2^{WT}$, compared with control cells expressing β-gal (Fig. 5, *B* and *C*). Consistently, myogenin expression also seemed to be enhanced in those expressing $SHP2^{C/S}$, compared with myoblasts expressing β-gal or $SHP2^{WT}$ (Fig. 5*B*). These data indicate that Gab1-SHP2 complex has an inhibitory effect on IGF-I-elicited myogenic differentiation through activation of SHP2 in C2C12 myoblasts.

siRNA-mediated Knockdown of Gab1 Enhances Myogenic Differentiation in C2C12 Myoblasts—To examine the effect of Gab1 protein depletion in C2C12 myoblasts, we performed siRNA-mediated Gab1 knockdown. Gab1 protein expression was reduced by 80% in the myoblasts transfected with Gab1-targeted siRNAs compared with control cells (Fig. 6*A*). On the second day after induction of differentiation, cells were immunostained with anti-MHC antibody. The extent of myogenic differentiation was enhanced in myoblasts transfected with Gab1-targeted siRNAs compared with control (Fig. 6*B*). Consistently, Western blot analysis also revealed a significant increase of MHC expression in myoblasts transfected with Gab1-targeted siRNAs compared with control (Fig. 6, *C* and *D*). Furthermore, the expression of myogenin was increased in myoblasts transfected with Gab1-targeted siRNAs (Fig. 6*C*). These data coincide with the results obtained via overexpression experiments using adenovirus vectors and suggest that Gab1 has an inhibitory role in the IGF-I-induced myogenic differentiation.

Moreover, we performed siRNAs-mediated SHP2 knockdown in C2C12 myoblasts. SHP2 protein expression was reduced by 70% in the myoblasts transfected with SHP2-targeted siRNAs compared with control cells (supplemental Fig. S2*A*). On the contrary to the results obtained by Gab1-targeted siRNAs experiments, SHP2 knockdown inhibited proliferation of C2C12 myoblasts. Therefore, we could not evaluate the myogenic differentiation in C2C12 myoblasts transfected with SHP2-targeted siRNAs (supplemental Fig. S2*B*).

IGF-I-induced Activation of ERK1/2 Is Regulated by Gab1-SHP2 Complex through Activation of SHP2 in C2C12 Myoblasts—To elucidate a potential mechanism how Gab1 is involved in IGF-I-mediated myogenic differentiation of C2C12 myoblasts, we examined the effects of adenovirus-mediated overexpression of $Gab1^{WT}$, $Gab1^{\Delta SHP2}$, and $Gab1^{\Delta p85}$ on the

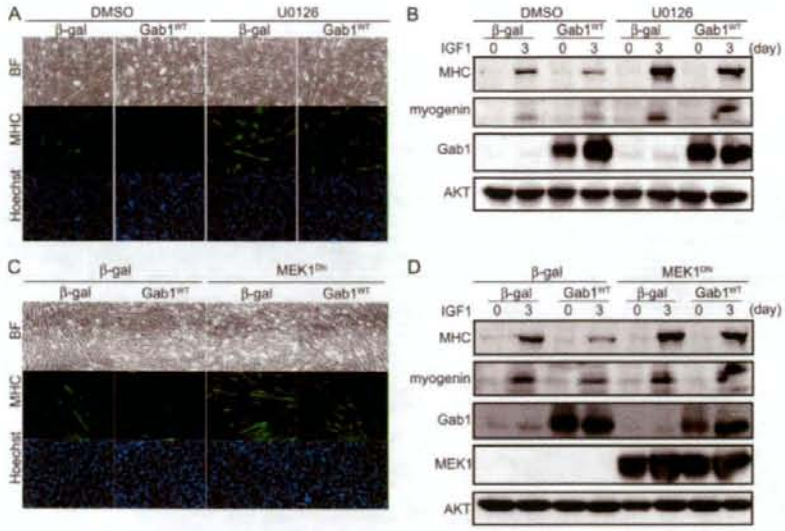

FIGURE 9. **ERK1/2 inhibition reverses the inhibitory effect of overexpression of Gab1^{WT} on IGF-I-induced myogenic differentiation.** *A*, C2C12 myoblasts were infected with adenovirus vectors overexpressing either β-gal or Gab1^{WT}. These cells were cultivated with or without a MEK1/2 inhibitor, U0126 (3 μM), under the differentiation medium containing 80 ng/ml IGF-I. On the third day after myogenic induction, the cells were immunostained with anti-MHC antibody and post-stained with Hoechst 33342 nuclear dye. Experiments were repeated three times with similar results. *B*, C2C12 cells overexpressing β-gal or Gab1^{WT} were cultured in the IGF-I-containing differentiation medium with or without U0126 (3 μM). Cell lysates were collected and subjected to Western blot analysis for analyzing the expression of MHC and myogenin. The membrane was reprobed with anti-Gab1 antibody for confirmation of adenoviral overexpression of Gab1. AKT was also checked as a loading control. *C*, C2C12 myoblasts were subjected to dual infection of adenovirus vectors expressing either β-gal or dominant-negative MEK1 (*MEK1^{DN}*) with Gab1^{WT}. On the third day after myogenic induction, the cells were immunostained with anti-MHC antibody and post-stained with Hoechst 33342 nuclear dye. Experiments were repeated three times with similar results. *D*, C2C12 myoblasts were subjected to dual infection of adenovirus vectors similarly to *B*. The cell lysates were collected and subjected to Western blot analysis for analyzing the expression of MHC and myogenin. The membrane was reprobed with anti-Gab1 and anti-MEK1 antibodies for confirmation of adenoviral overexpression of Gab1 and MEK1. AKT was also checked as a loading control. Experiments were repeated three times with similar results.

IGF-I-dependent signaling pathways downstream of Gab1. IGF-I induced activation of ERK1/2 and AKT in control myoblasts expressing β-gal. IGF-I-induced activation of ERK1/2 was significantly augmented in myoblasts overexpressing Gab1^{WT} or Gab1$^{\Delta p85}$ compared with control myoblasts expressing β-gal. On the other hand, activation of ERK1/2 was significantly reduced in myoblasts expressing Gab1$^{\Delta SHP2}$ (Fig. 7, *A* and *B*). On the other hand, activation of ERK1/2 was not changed in myoblasts expressing Gab2$^{\Delta SHP2}$ compared with control myoblasts expressing β-gal (supplemental Fig. S1*D*). These data indicate that Gab1 plays a critical role in IGF-I-induced ERK1/2 activation through interaction with SHP2 in C2C12 myoblasts.

IGF-I-induced AKT activation was almost comparable in myoblasts expressing β-gal, Gab1^{WT}, or Gab1$^{\Delta SHP2}$. On the contrary, activation of AKT seemed to be enhanced in cells overexpressing Gab1 $^{\Delta p85}$, compared with the other three groups (Fig. 7*B*). These data indicate that Gab1 might have a competitive role for sequestering p85 in the cytoplasm from other scaffolding adaptor proteins such as IRS-1.

To confirm the requirement of SHP2 activity for activation of ERK1/2 upon IGF-I stimulation, we examined the effects of adenovirus-mediated overexpression of SHP2^{WT} or SHP2$^{C/S}$ on ERK1/2 activation. IGF-I-induced activation of ERK1/2 was comparable in myoblasts overexpressing SHP2^{WT} and those expressing β-gal, but almost inhibited in cells overexpressing SHP2$^{C/S}$ compared with control (Fig. 8, *A* and *B*). On the other hand, activation of AKT was almost comparable among the three groups (Fig. 8, *A* and *B*). These findings indicate that SHP2 catalytic activity is indispensable for activation of ERK1/2 after stimulation with IGF-I in C2C12 myoblasts. Taken together, our findings indicate that IGF-I activates ERK1/2 via complex formation of Gab1 with SHP2 and activation of SHP2 in C2C12 myoblasts.

Gab1-SHP2-ERK1/2-signaling Pathway Is an Inhibitory Axis of IGF-I-dependent Myogenic Differentiation in C2C12 Myoblasts—It has been reported that ERK1/2 has an inhibitory role for myogenic differentiation of mesenchymal cells to date (3, 10). Therefore, we assumed that Gab1-SHP2 complex might have the inhibitory effects on myogenic differentiation via activation of ERK1/2. To confirm the inhibitory role of ERK1/2 downstream of Gab1-SHP2 complex, myoblasts overexpressing Gab1^{WT} were treated with or without a MEK1/2 inhibitor, U0126, before inducing myoblasts into myogenic differentiation in the presence of IGF-I. U0126 enhanced IGF-I-induced up-regulation of MHC and myogenin in control myoblasts expressing β-gal (Fig. 9, *A* and *B*). Furthermore, U0126 reversed the inhibitory effect of Gab1^{WT} overexpression on up-regulation of MHC and myogenin (Fig. 9, *A* and *B*). We also confirmed that adenovirus-mediated overexpression of dominant-negative MEK1 (MEK1^{DN}) reversed the inhibitory effect of Gab1^{WT} overexpression on IGF-I-induced myogenic differentiation (Fig. 9, *C* and *D*). These findings suggest that Gab1 inhibits IGF-I-dependent myogenesis through activating MEK1/2-ERK1/2 pathway.

Finally, we examined the effect of adenoviral overexpression of constitutively active MEK1 (MEK1^{CA}). Overexpression of MEK1^{CA} repressed the enhanced myogenic differentiation observed in myoblasts overexpressing Gab1$^{\Delta SHP2}$ (Fig. 10, *A* and *B*). Collectively, interaction of Gab1 with SHP2 negatively regulates IGF-I-dependent myogenic differentiation in C2C12 myoblasts via activation of the MEK1/2-ERK1/2 pathway (Fig. 11).

DISCUSSION

In this study, we investigated the role of Gab1 in skeletal muscle differentiation. To our knowledge, this study demon-

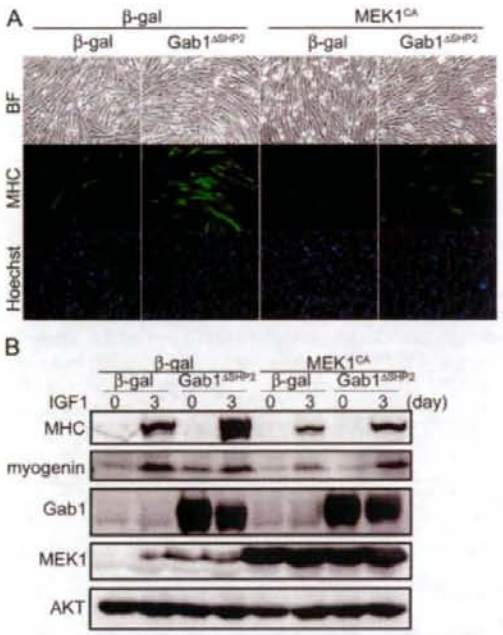

FIGURE 10. **Overexpression of constitutively active MEK1 abrogates the promoting effect of Gab1$^{\Delta SHP2}$ on myogenic differentiation in C2C12 cells.** *A*, C2C12 myoblasts were subjected to dual infection of adenovirus vectors expressing either β-gal or constitutively active MEK1 (MEK1^{CA}) with Gab1$^{\Delta SHP2}$. On the third day after myogenic induction, the cells were immunostained with anti-MHC antibody and post-stained with Hoechst 33342 nuclear dye. Overexpression of MEK1^{CA} in C2C12 significantly repressed the promoting effect of the overexpression of Gab1$^{\Delta SHP2}$ on IGF-I-induced myogenic differentiation. *B*, C2C12 myoblasts were subjected to dual infection of adenovirus vectors similar to *A*. The cell lysates were collected from 3.5-cm dishes and subjected to Western blot analysis. Dual overexpression of MEK1^{CA} with Gab1$^{\Delta SHP2}$ repressed the promoting effect of Gab1$^{\Delta SHP2}$ on the induction of MHC protein. Experiments were repeated three times with similar results.

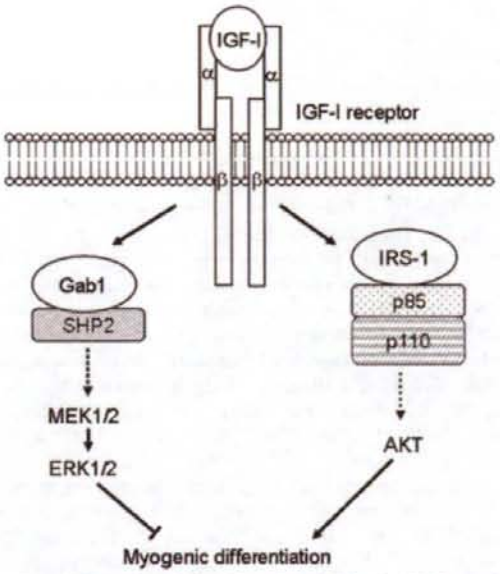

FIGURE 11. **Schematic models of the roles of Gab1 in IGF-I-dependent myogenic differentiation.** IGF-I induces tyrosine phosphorylation of Gab1 and subsequent association of Gab1 with SHP2. Gab1-SHP2 complex plays a critical role in activation of ERK1/2 in C2C12 myoblasts. Furthermore, Gab1-SHP2 complex negatively regulates myogenic differentiation via activation of MEK1/2-ERK1/2 pathway. On the other hand, IGF-I stimulation also induced tyrosine phosphorylation of IRS-I and subsequent association with p85 PI3K subunit. IRS-I-p85 complex formation has been reported to be indispensable for PI3K-AKT signaling, which might result in promotion of myogenic differentiation.

strates for the first time that Gab1 has an inhibitory role in IGF-I-induced myogenic differentiation through activating SHP2-MEK1/2-ERK1/2 signaling pathway.

IGF-I induced complex formation of Gab1 with SHP2 in C2C12 myoblasts. It has been reported that Gab1 undergoes dramatic tyrosine-dephosphorylation upon changing growth medium to differentiation medium containing 2% HS in C2C12 cells (42). This finding indicated that Gab1 might have a key role in myogenic differentiation. Recently, it has been reported that Gab1 itself is a substrate of SHP2 (39). Furthermore, it has been reported that phosphorylation of ERK1/2 decreases while phosphorylation of AKT increases during differentiation with either insulin or 2% HS (9). Therefore, tyrosine dephosphorylation of Gab1 and subsequent dissociation of SHP2 from dephosphorylated Gab1 might be essential steps for the diminution of ERK1/2 activity during myogenic differentiation.

The Gab1-SHP2 complex formation is indispensable for IGF-I-induced activation of ERK1/2. It has been reported that Gab1-SHP2 interaction has an essential role for ERK1/2 activation downstream of EGF family/ErbB receptor signaling or hepatocyte growth factor/c-Met signaling (20–23). Furthermore, the recent study creating liver-specific Gab1 knock-out mice also demonstrated that Gab1 is required for both insulin-elicited ERK1/2 activation and subsequent inhibition of IRS-1-PI3K-AKT signaling (34). Here, we demonstrated that overexpression of Gab1$^{\Delta SHP2}$, which is incapable of associating with SHP2, repressed IGF-I-dependent activation of ERK1/2 in C2C12 myoblasts. In a similar context, SHP2 itself has been reported to have crucial roles for ERK1/2 activation downstream of various growth factors, including IGF-I (24, 43–46). We also observed that overexpression of phosphatase-inactive SHP2 (SHP2$^{C/S}$) inhibited IGF-I-dependent activation of ERK1/2 in C2C12 myoblasts. These findings demonstrate that Gab1-SHP2 complex formation is requisite for both activation of SHP2 itself and ERK1/2 upon IGF-1 stimulation in C2C12 myoblasts. Because the mechanism how SHP2 regulates receptor tyrosine kinase-mediated ERK1/2 activation remains controversial (18, 19), further analyses are needed for uncovering the mechanism how Gab1-SHP2 complex regulates IGF-I-induced activation of ERK1/2.

The Gab1-SHP2 complex exerts an inhibitory effect on the IGF-I-induced myogenic differentiation through activation of ERK1/2. IGFs have been reported to stimulate both proliferation and differentiation of skeletal muscle cells in culture (3, 4). IGFs activate two major cytoplasmic signaling pathways, PI3K-AKT cascade and Raf-MEK1/2-ERK1/2 MAPK cascade. The former has been reported to have positive effects on myogenesis, and the latter MAPK-signaling cascade has been reported to have detrimental effects on the myogenic differentiation

induced by insulin or IGFs (3, 9, 10). SHP2 has been also reported to play an inhibitory role for myogenic differentiation in the presence of fibroblast growth factor 2 (FGF2) in C2C12 myoblasts partly in an ERK1/2-dependent manner (44). We found that IGF-I-induced myogenic differentiation was inhibited by overexpression of either $Gab1^{WT}$ or $Gab1^{\Delta p85}$, but not by that of $SHP2^{WT}$. In addition, IGF-I-induced ERK1/2 activation in C2C12 myoblasts was enhanced by overexpression of either $Gab1^{WT}$ or $Gab1^{\Delta p85}$, but not by that of $SHP2^{WT}$. SHP2 can be specifically activated through binding directly with tyrosine-phosphorylated docking proteins such as Gab1 or FRS2α (18), suggesting that a sufficient amount of Gab1 is required to fully activate SHP2 by binding with SHP2 and that an insufficient amount of endogenous Gab1 might be the major limiting factor in overexpressed $SHP2^{WT}$-mediated myogenic differentiation. Collectively, these data suggest that Gab1 is a crucial negative regulator for IGF-I-dependent myogenic differentiation through activation of the SHP2-MEK1/2-ERK1/2 signaling pathway (Fig. 10).

The migration of muscle progenitor cells into the limb anlage from somites is strongly impaired in Gab1-knock-out embryos similarly in c-Met-knock-out mice (32). Furthermore, it has been reported that the knock-in mice, which carry mutant Gab1 incapable of binding with SHP2, displayed quite similar defects in migration of muscle progenitor cells from somites into the limb anlage during embryogenesis as observed in Gab1-knock-out mice (29). In clear contrast, the knock-in mice, which carry mutant Gab1 incapable of binding either Grb2 or c-Met, did not show any defects in migration of muscle progenitor cells, suggesting the specific role of Gab1-SHP2 complex in the migration of muscle progenitor cells (29). These previous data coincide with our findings that Gab1-SHP2 interaction has an inhibitory effect on IGF-I-induced myogenic differentiation. Taken together, Gab1 might play a key role not only for inhibition of myogenesis but also for maintenance of the undifferentiated state of mesenchymal cells through activation of SHP2.

Although the PI3K-AKT signaling pathway is central to IGF-I-dependent signaling and myogenic differentiation, our data demonstrate that the diminution of ERK1/2 activity is a prerequisite for IGF-I-induced myogenesis. IGFs promote skeletal muscle differentiation through PI3K-AKT-dependent signaling pathway (3, 6, 7, 47–49). It has been reported that the activity of AKT increased during myogenic differentiation under cultivation in 2% HS or IGF-I-containing differentiation medium (9). We found that overexpression of $Gab1^{\Delta p85}$ in C2C12 myoblasts resulted in enhanced activation of AKT upon stimulation with IGF-I, compared with those overexpressing $Gab1^{WT}$ or $Gab1^{\Delta SHP2}$. However, overexpression of $Gab1^{\Delta p85}$ did not enhance, but repressed IGF-I-induced myogenic differentiation to a similar extent to $Gab1^{WT}$. In clear contrast, overexpression of $Gab1^{\Delta SHP2}$ significantly enhanced IGF-I-induced myogenic differentiation compared with control. These findings indicate that myogenic differentiation requires the diminution of Gab1-SHP2-ERK1/2 signaling pathway prior to full activation of PI3K-AKT signaling pathway. It has been reported that the blockade of ERK1/2 signaling pathway enhances myogenic differentiation (3, 8–10). Inhibition of the ERK1/2 pathway has been reported to up-regulate Mirk/dyrk1B, a RhoA-dependent serine/threonine kinase that positively regulates skeletal muscle differentiation and inhibits apoptosis of myoblasts (50). Mirk/dyrk1B might be one of the candidate molecules through which ERK1/2 exerts an inhibitory effect on skeletal muscle differentiation.

In conclusion, the present study reveals that Gab1-SHP2 interaction exerts an inhibitory effect on IGF-I-dependent myogenic differentiation via activation of ERK1/2 signaling pathway.

Acknowledgments—We are grateful to S. Kawashima (Kobe University) for adenovirus vectors expressing dominant-negative MEK1 ($MEK1^{DN}$) and constitutively active MEK1 ($MEK1^{CA}$); T. Saito and S. Yamasaki (RIKEN Research Center for Allergy and Immunology) for $Gab2^{\Delta SHP2}$ cDNA; J. T. Pearson for his critical reading of this manuscript; Yuko Matsuura and Masako Suto for secretarial work; and Maki Yoshida, Y Mizushima, and Manami Sone for their technical assistance.

REFERENCES

1. Bach, L. A., Salemi, R., and Leeding, K. S. (1995) *Endocrinology* **136,** 5061–5069
2. Ewton, D. Z., Roof, S. L., Magri, K. A., McWade, F. J., and Florini, J. R. (1994) *J. Cell Physiol.* **161,** 277–284
3. Coolican, S. A., Samuel, D. S., Ewton, D. Z., McWade, F. J., and Florini, J. R. (1997) *J. Biol. Chem.* **272,** 6653–6662
4. Florini, J. R., Ewton, D. Z., and Coolican, S. A. (1996) *Endocr. Rev.* **17,** 481–517
5. White, M. F. (2003) *Science* **302,** 1710–1711
6. Kaliman, P., Vinals, F., Testar, X., Palacin, M., and Zorzano, A. (1996) *J. Biol. Chem.* **271,** 19146–19151
7. Kaliman, P., Canicio, J., Shepherd, P. R., Beeton, C. A., Testar, X., Palacin, M., and Zorzano, A. (1998) *Mol. Endocrinol.* **12,** 66–77
8. Bennett, A. M., and Tonks, N. K. (1997) *Science* **278,** 1288–1291
9. de Alvaro, C., Martinez, N., Rojas, J. M., and Lorenzo, M. (2005) *Mol. Biol. Cell* **16,** 4454–4461
10. Tortorella, L. L., Milasincic, D. J., and Pilch, P. F. (2001) *J. Biol. Chem.* **276,** 13709–13717
11. Gu, H., and Neel, B. G. (2003) *Trends Cell Biol.* **13,** 122–130
12. Nishida, K., and Hirano, T. (2003) *Cancer Sci.* **94,** 1029–1033
13. Holgado-Madruga, M., Emlet, D. R., Moscatello, D. K., Godwin, A. K., and Wong, A. J. (1996) *Nature* **379,** 560–564
14. Montagner, A., Yart, A., Dance, M., Perret, B., Salles, J. P., and Raynal, P. (2005) *J. Biol. Chem.* **280,** 5350–5360
15. Nishida, K., Yoshida, Y., Itoh, M., Fukada, T., Ohtani, T., Shirogane, T., Atsumi, T., Takahashi-Tezuka, M., Ishihara, K., Hibi, M., and Hirano, T. (1999) *Blood* **93,** 1809–1816
16. Takahashi-Tezuka, M., Yoshida, Y., Fukada, T., Ohtani, T., Yamanaka, Y., Nishida, K., Nakajima, K., Hibi, M., and Hirano, T. (1998) *Mol. Cell Biol.* **18,** 4109–4117
17. Weidner, K. M., Di Cesare, S., Sachs, M., Brinkmann, V., Behrens, J., and Birchmeier, W. (1996) *Nature* **384,** 173–176
18. Neel, B. G., Gu, H., and Pao, L. (2003) *Trends Biochem. Sci.* **28,** 284–293
19. Tiganis, T., and Bennett, A. M. (2007) *Biochem. J.* **402,** 1–15
20. Cunnick, J. M., Dorsey, J. F., Munoz-Antonia, T., Mei, L., and Wu, J. (2000) *J. Biol. Chem.* **275,** 13842–13848
21. Cunnick, J. M., Mei, L., Doupnik, C. A., and Wu, J. (2001) *J. Biol. Chem.* **276,** 24380–24387
22. Nakaoka, Y., Nishida, K., Fujio, Y., Izumi, M., Terai, K., Oshima, Y., Sugiyama, S., Matsuda, S., Koyasu, S., Yamauchi-Takihara, K., Hirano, T., Kawase, I., and Hirota, H. (2003) *Circ. Res.* **93,** 221–229
23. Schaeper, U., Gehring, N. H., Fuchs, K. P., Sachs, M., Kempkes, B., and Birchmeier, W. (2000) *J. Cell Biol.* **149,** 1419–1432

24. Cunnick, J. M., Meng, S., Ren, Y., Desponts, C., Wang, H. G., Djeu, J. Y., and Wu, J. (2002) *J. Biol. Chem.* **277,** 9498–9504
25. Dance, M., Montagner, A., Yart, A., Masri, B., Audigier, Y., Perret, B., Salles, J. P., and Raynal, P. (2006) *J. Biol. Chem.* **281,** 23285–23295
26. Jin, Z. G., Wong, C., Wu, J., and Berk, B. C. (2005) *J. Biol. Chem.* **280,** 12305–12309
27. Laramee, M., Chabot, C., Cloutier, M., Stenne, R., Holgado-Madruga, M., Wong, A. J., and Royal, I. (2007) *J. Biol. Chem.* **282,** 7758–7769
28. Mattoon, D. R., Lamothe, B., Lax, I., and Schlessinger, J. (2004) *BMC. Biol.* **2,** 24
29. Schaeper, U., Vogel, R., Chmielowiec, J., Huelsken, J., Rosario, M., and Birchmeier, W. (2007) *Proc. Natl. Acad. Sci. U. S. A.* **104,** 15376–15381
30. Rodrigues, G. A., Falasca, M., Zhang, Z., Ong, S. H., and Schlessinger, J. (2000) *Mol. Cell Biol.* **20,** 1448–1459
31. Itoh, M., Yoshida, Y., Nishida, K., Narimatsu, M., Hibi, M., and Hirano, T. (2000) *Mol. Cell Biol.* **20,** 3695–3704
32. Sachs, M., Brohmann, H., Zechner, D., Muller, T., Hulsken, J., Walther, I., Schaeper, U., Birchmeier, C., and Birchmeier, W. (2000) *J. Cell Biol.* **150,** 1375–1384
33. Nakaoka, Y., Nishida, K., Narimatsu, M., Kamiya, A., Minami, T., Sawa, H., Okawa, K., Fujio, Y., Koyama, T., Maeda, M., Sone, M., Yamasaki, S., Arai, Y., Koh, G. Y., Kodama, T., Hirota, H., Otsu, K., Hirano, T., and Mochizuki, N. (2007) *J. Clin. Invest.* **117,** 1771–1781
34. Bard-Chapeau, E. A., Hevener, A. L., Long, S., Zhang, E. E., Olefsky, J. M., and Feng, G. S. (2005) *Nat. Med.* **11,** 567–571
35. Yamasaki, S., Nishida, K., Yoshida, Y., Itoh, M., Hibi, M., and Hirano, T. (2003) *Oncogene* **22,** 1546–1556
36. Becker, T. C., Noel, R. J., Coats, W. S., Gomez-Foix, A. M., Alam, T., Gerard, R. D., and Newgard, C. B. (1994) *Methods Cell Biol.* **43,** 161–189
37. Ueyama, T., Kawashima, S., Sakoda, T., Rikitake, Y., Ishida, T., Kawai, M., Yamashita, T., Ishido, S., Hotta, H., and Yokoyama, M. (2000) *J. Mol. Cell Cardiol.* **32,** 947–960
38. Sarbassov, D. D., and Peterson, C. A. (1998) *Mol. Endocrinol.* **12,** 1870–1878
39. Zhang, S. Q., Tsiaras, W. G., Araki, T., Wen, G., Minichiello, L., Klein, R., and Neel, B. G. (2002) *Mol. Cell Biol.* **22,** 4062–4072
40. Meng, S., Chen, Z., Munoz-Antonia, T., and Wu, J. (2005) *Biochem. J.* **391,** 143–151
41. Yamasaki, S., Nishida, K., Hibi, M., Sakuma, M., Shiina, R., Takeuchi, A., Ohnishi, H., Hirano, T., and Saito, T. (2001) *J. Biol. Chem.* **276,** 45175–45183
42. Kontaridis, M. I., Liu, X., Zhang, L., and Bennett, A. M. (2001) *J. Cell Sci.* **114,** 2187–2198
43. Ivins, Z. C., Kontaridis, M. I., Fornaro, M., Feng, G. S., and Bennett, A. M. (2004) *J. Cell Physiol.* **199,** 227–236
44. Kontaridis, M. I., Liu, X., Zhang, L., and Bennett, A. M. (2002) *Mol. Cell Biol.* **22,** 3875–3891
45. Shi, Z. Q., Yu, D. H., Park, M., Marshall, M., and Feng, G. S. (2000) *Mol. Cell Biol.* **20,** 1526–1536
46. Shi, Z. Q., Lu, W., and Feng, G. S. (1998) *J. Biol. Chem.* **273,** 4904–4908
47. Jiang, B. H., Zheng, J. Z., Aoki, M., and Vogt, P. K. (2000) *Proc. Natl. Acad. Sci. U. S. A.* **97,** 1749–1753
48. Jiang, B. H., Zheng, J. Z., and Vogt, P. K. (1998) *Proc. Natl. Acad. Sci. U. S. A.* **95,** 14179–14183
49. Jiang, B. H., Aoki, M., Zheng, J. Z., Li, J., and Vogt, P. K. (1999) *Proc. Natl. Acad. Sci. U. S. A.* **96,** 2077–2081
50. Deng, X., Ewton, D. Z., Pawlikowski, B., Maimone, M., and Friedman, E. (2003) *J. Biol. Chem.* **278,** 41347–41354